

STATUS OF THE HIGH-CURRENT EBIS CHARGE BREEDER FOR THE FACILITY FOR RARE ISOTOPE BEAMS*

H.J. Son[†], A. C.C. Villari, A. Henriques, C. Knowles, Facility for Rare Isotope Beam (FRIB),
 Michigan State University (MSU), East Lansing, USA
 A. Lapierre, D. Crisp, S. Nash, National Superconducting Cyclotron Laboratory (NSCL),
 Michigan State University (MSU), East Lansing, USA
 E. N. Beebe, Brookhaven National Laboratory, Upton, USA

Abstract

The ReA post-accelerator of the National Superconducting Cyclotron Laboratory (NSCL) at Michigan State University includes an Electron-Beam Ion Trap (EBIT) operating as a charge breeder. The Facility for Rare Isotope Beams (FRIB) is being implemented. After completion, rare-isotopes beam rates are expected to exceed in some case 10^{10} particles per second (pps). The charge capacity of the ReA EBIT is insufficient to handle those rates. Therefore, parts of the TEST EBIS from the Brookhaven National Laboratory (BNL) were transferred to the NSCL to build a High-Current Electron-Beam Ion Source (HCEBIS). The HCEBIS features an electron gun that can provide a current up to 4 A for an estimated trap charge capacity of 10^{11} elementary charges. This paper presents the HCEBIS specifications, electron-beam current measurements to test its cathode, and simulation results for its implementation in the ReA post-accelerator. It also presents charge-capacity measurements conducted with the ReA EBIT that demonstrate that the HCEBIS will be able to handle beam rates of more than 10^{10} pps.

INTRODUCTION

The ReA post-accelerator [1] of the National Superconducting Cyclotron Laboratory (NSCL) at Michigan State University includes an Electron-Beam Ion Trap (EBIT) operating as a charge breeder. At the NSCL, Rare-Isotope Beams (RIB) are currently produced by fast-projectile fragmentation and fission with the Coupled-Cyclotron Facility (CCF). After production, these beams are then separated in-flight and thermalized in a helium gas cell before being transported to the ReA post-acceleration for charge breeding and then reacceleration with a linear accelerator up to several MeV/u for the nuclear physics program. The Facility for Rare Isotope Beams, FRIB, is being implemented based on a 400-kW heavy-ion linear accelerator (LINAC) [2]. After the transition from CCF-to-the FRIB LINAC, the production yield of rare isotopes will significantly increase. In some cases, rates are expected to exceed 10^{10} particles/s (pps). In addition, the user community for the Separator for Capture Reactions (SECAR) recoil separator [3] has requested stable-isotope ion beams with rates up to 10^{10} pps.

The ReA EBIT [4] has a limited charge capacity of 10^{10} elementary ($1+$) charges, which is insufficient to efficiently

charge breed to high charge states RIB of high rates from FRIB. To increase the charge capacity of the ReA charge breeder, a new High-Current Electron-Beam Ion Source (HCEBIS) is being built. The HCEBIS uses the “backbones” of the TEST EBIS [5], which was transferred from the Brookhaven National Laboratory (BNL) in 2018. The HCEBIS can operate with an electron-beam current exceeding 4 A and has a trap length of 0.7m, allowing the device to deliver highly charged ion beams of intensities expected to be more than 10^{10} ions per second. The specifications of the HCEBIS are summarized in Table 1.

Table 1: HCEBIS Specifications

| | |
|-------------------------------|------------------------------|
| Electron-beam current | ≤ 4 A |
| Electron-beam energy | ≤ 20 keV |
| Magnetic field (trap center) | ≤ 5 T |
| Electron-beam current density | ≤ 200 A/cm ² |
| Trap length | 0.7 m |

The assembly of the HCEBIS has recently been completed from the electron gun to the collector, as shown in Fig. 1. The normal conducting solenoids were installed at the electron gun and the collector side. Preliminary vacuum tests for the electron gun and trap section have been completed. The control system is currently being implemented.

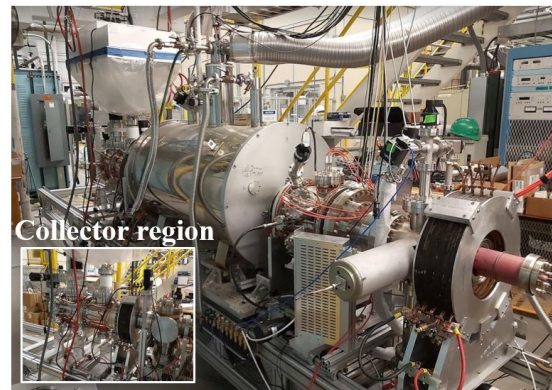


Figure 1: Assembled HCEBIS from the electron gun to the collector.

CATHODE TEST

The HCBIS will use for operation a magnetically immersed electron gun providing up to 4 A in current. The magnetic field near the cathode can suppress large radial beam oscillations, therefore the cathode is immersed in the

* Work supported by the National Science Foundation under Grant No. PHY-1565546.

[†]son@frib.msu.edu

magnetic field of approximately 0.15 T [6]. The dispenser cathode material is made of lanthanum hexaboride (LaB6), and the cathode diameter is 9.2 mm. The LaB6 cathode currently installed was tested without magnetic fields in a test configuration.

The electron-beam is produced from the cathode by an applied high voltage onto the anode. The emitted electrons diverge due to the absence of magnetic field near the cathode. They are then accelerated and intercepted by the anode, as illustrated in Fig. 2. A pulsing circuit including a fast switch was employed to produce short electron-beam pulses of less than 10 μ s to minimize the beam power on the anode and minimize the charge required to be stored in the pulsing circuit capacitors. In the turn-off period of the switch, the anode was biased to -100 V to suppress the thermal electron emission from the cathode. The pulsed emitted electron current was measured using a current transducer (Pearson, Current Monitor Model 110). Figure 2 presents the result of an electron-beam simulation in the test configuration using TRAK (see next section) and a diagram of the pulsing circuit.

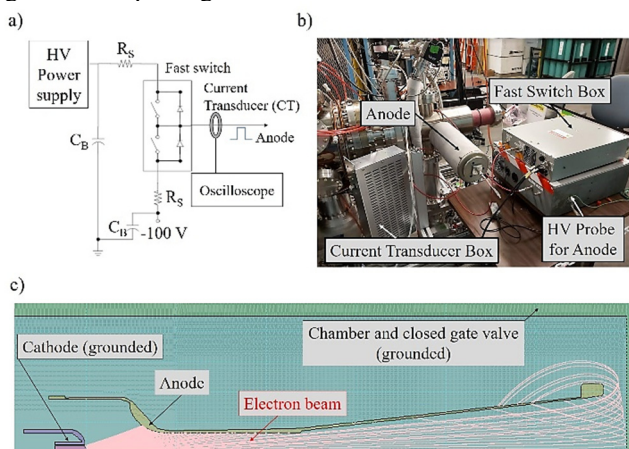


Figure 2: a) Pulsing circuit diagram, b) a photo of the experimental set-up, and c) TRAK simulation result.

Figure 3 shows the electron-beam current as function of the anode voltage with the cathode on ground potential. The anode voltage was varied from 0 V to 10 kV. With the low heater power, the emission current is limited by the temperature of the cathode surface. For higher heater power, the emitted beam current becomes only limited by the electron-beam space-charge. The I-V (current vs. voltage) curve can then be reasonably fitted with the Child-Langmuir law. The emission current is 1.12 A at the anode voltage of 10 kV with 137.4 W of heater power, corresponding to a perveance value of $1.12 \times 10^{-6} \text{ A/V}^{3/2}$. With the heater power of 114.3 W and 137.4 W, the emission current values were the same. The emitted beam current was already limited by electron-beam space-charge with the heater power of 114.3 W. The dash line in Fig. 3 shows a simulated I-V curve having a perveance of $1.45 \times 10^{-6} \text{ A/V}^{3/2}$. According to the perveance value measured at high heater power, the required potential difference between the cathode and the anode is 23.3 kV to obtain the electron-beam current of 4 A.

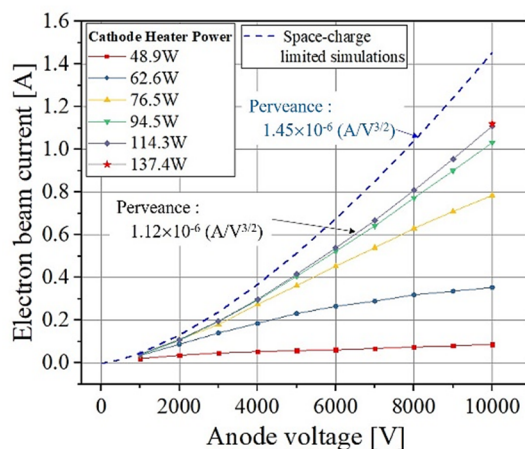


Figure 3: I-V curve of the cathode with different cathode heater powers.

HCEBIS BEAM SIMULATIONS

Beam simulations are a crucial step to verify the characteristics of the HCEBIS system to be integrated into ReA. An electron gun (e-gun) produces an electron-beam with small energy spread (quasi-mono-energetic). The electron-beam is then transported to the trap and compressed by a high magnetic field in its center. The compressed electron-beam plays two roles in the EBIS charge breeder. The electron-beam space-charge due to the compressed electron-beam, generates a strong radial potential well that traps ions radially. Trapped ions are quickly ionized to high charge states with the high current density of the electron-beam which generates a narrow charge-state distribution, increasing the breeding efficiency. Important characteristics are the electron-beam emission from the e-gun, electron-beam transport from the cathode to the collector, ion trap capacity, and current density distribution in the trap. The beam acceptance of the HCEBIS and emittance of the HCEBIS are also significant characteristics. Simulations have been conducted using Field Precision programs: ES-TAT, PERMAG, and TRAK [7].

Electron-Beam Simulation

The simulation domain was two dimensional, and a single domain was used from the cathode to the collector to prevent discontinuities. All components in the simulation were assumed to be ideally axi-symmetric. Figure 4. a) shows the magnetic field and electric potential distributions in the HCEBIS along the beam axis. The cathode surface is positioned at $z=0$. The axial magnetic field near the cathode is approximately 0.15T and the potential difference between the cathode and the anode is near 20.6 kV. With this potential difference, the emitted beam current converged to 4 A.

The radial mesh size near the beam axis was set 10 times smaller than the outside mesh size for accurate beam trajectory calculations. The time step was set to $5 \times 10^{-14} \text{ s}$. The electron-beam was transported from the cathode to the collector, as shown in Fig. 4. b). The electron-beam radius varied with the magnetic field along the beam axis and was

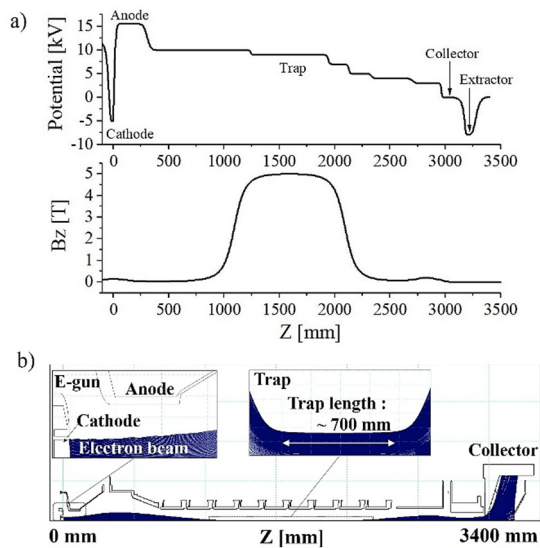


Figure 4: a) Axial magnetic field and electric potential distributions along the beam axis, and b) electron-beam trajectories from the cathode to the collector.

compressed by the magnetic field of 5T at the trap center. Figure 5 shows the radial electron-beam current density in the trap area. These current density values were averaged values of 40 axial points along the trap length. The current density is around 192 A/cm². The electron-beam radius according to the beam current density is estimated to be around 0.8 mm.

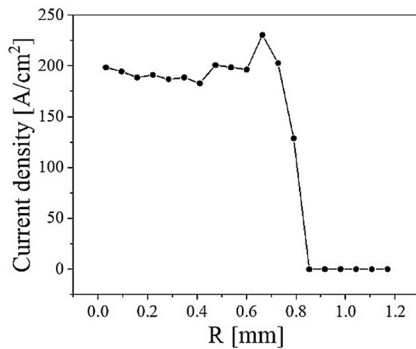


Figure 5: Electron-beam current density in the trap center (5-T magnetic field).

For an immersed electron gun of low space-charge potential, the electron-beam radius at an arbitrary z position can be expressed as [8]

$$r_z = r_{cathode} \sqrt{\frac{B_{cathode}}{B_z}} \quad (1)$$

where $r_{cathode}$ is the cathode radius, $B_{cathode}$ is the axial magnetic field at the cathode surface, and B_z is the axial magnetic field at the z position, respectively. The beam radius at the trap center can be calculated with Eq. (1) as 0.796 mm with the cathode magnetic field of 0.15T and the trap magnetic field of 5T. This value agrees well with the radius obtained from the simulations.

The theoretical charge capacity of an EBIS is given by [9]

$$C_{trap} = \frac{1.05 \times 10^{13} \times I_e \times L}{\sqrt{E_e}} \times f \quad (2)$$

It follows that the charge capacity of the HCEBIS is expected to be 2.4×10^{11} elementary charges, assuming a trap length (L), electron-beam current (I_e), compensation ratio (f), and electron-beam energy (E_e) of 0.7 m, 4 A, 1, and 15 keV, respectively. This capacity is sufficient to charge breed injected beam rates of 10^{10} pps of light ions. For instance, the HCEBIS could confine 3×10^{10} particles of Ne^{8+} . Even if losses are considered in the HCEBIS and during transport through the ReA LINAC, beam intensities of more than 10^{10} pps could be delivered to experimental facilities.

Beam Acceptance of the HCEBIS

The ReA EBIT in operation employs a Pierce-type gun in a magnetically semi-immersed configuration [10, 11]. The electron-beam size in the ReA EBIT trap is significantly smaller than that of a magnetically immersed electron gun. Hence, the acceptance of the ReA EBIT is smaller than the HCEBIS acceptance. ReA includes a beam cooler-buncher (BCB) [4] for pulsed injection into the ReA EBIT. Although for injected beams of low intensity the BCB beam emittance is smaller than the EBIT acceptance, its emittance is expected to significantly increase for high-intensity beams. Evaluating the acceptance of the HCEBIS is needed to understand its limits in capturing high-intensity pulsed beams from the BCB [12].

Figure 6 shows axial electric potential distributions. The dash-dot line represents the distribution without the electron-beam space-charge. When the electron-beam is on, the electron-beam space-charge changes the spatial electric potential, as shown by the solid line. This potential distribution with the electron-beam space-charge was obtained in the previous electron-beam simulation and was used for the injection simulation.

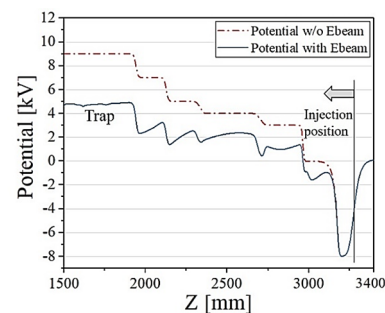


Figure 6: Axial electric potential distributions for the injection simulation with electron-beam current of 4 A and electron-beam energy of 14 keV.

A Ne^{1+} beam is injected from the injection position located at the end of the extractor shown in Fig. 6 and Fig. 7. The injected Ne^{1+} beam stops in the middle of the trap at $z = 1500$ mm. The initial injected ions were distributed uniformly in a $x-x'$ phase-space rectangular that covered a $30\text{mm} \times 150\text{mrad}$ domain. The number of ions was 18272. The initial kinetic energy was set to 12 keV, and the averaged kinetic energy in the trap was around 0.9 keV. The accepted ion beam trajectory within the electron-beam in the trap is shown in Fig. 7. As shown in Fig. 8, the injected

ions have a different overlap factor ($f_{overlap}$) with the electron-beam. Some ions are moving within the electron-beam over the whole trap length. In this case, the overlap factor is 1. Other ions partially overlaps with the electron-beam. Most, however, are not overlapping with the electron-beam or being accepted into the trap area (zero overlap factor).

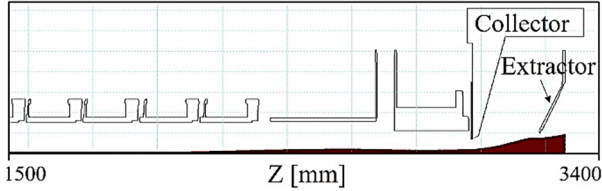


Figure 7: Injected ion beam trajectories with overlap factor of 1.

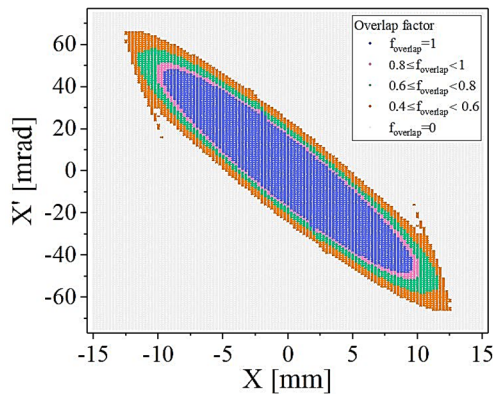


Figure 8: Acceptance ellipse with different overlap factor with the electron-beam: $f_{overlap}=1$ represents a full overlap.

The overlap factor is depended on the initial radial position and angle. All particle trajectories were tracked, and the overlap factors were obtained for each ion. The acceptance ellipse with a different overlap factor is shown in Fig. 8. The 4 times root-mean-square (4-RMS) acceptance for ions having an overlap factor 1 is 167 mm·mrad. The 4-RMS acceptance for all accepted ions having different overlapping factor is 518 mm·mrad. The 4-RMS acceptance was obtained by calculating 4-RMS emittance of the injected ions accepted with different overlap factors using the expression [13]:

$$\varepsilon_{4-RMS} = 4 \cdot \sqrt{\overline{x^2 \cdot x'^2} - \overline{x} \cdot \overline{x'}^2} \text{ mm} \cdot \text{mrad} \quad (3)$$

Wenander *et al.*, [9] obtained an analytical expression to estimate the maximum geometrical acceptance of an EBIS:

$$\alpha_{max} = x_{outmax} x'_{outmax} = \frac{r_{ebeam}}{\sqrt{2U_{ext}}} \cdot \left(Br_{ebeam} \sqrt{\frac{q}{m}} + \sqrt{\frac{qB^2 r_{ebeam}^2}{4m} + \frac{\rho_l}{2\pi\epsilon_0}} \right) \quad (4)$$

where r_{ebeam} , U_{ext} , q , m and ρ_l represent the electron-beam radius, ion injection potential, ion charge, ion mass and electron-beam charge per meter, respectively. The equation accounts for the electron-beam space-charge potential and was derived for ions having an overlap factor of 1 with a

non-compensated electron-beam. From this equation, the HCEBIS maximum geometrical acceptance is 217 mm·mrad with the trap magnetic field at 5T and the electron-beam radius of 0.796 mm in the trap.

An acceptance comparison with the TEST EBIS is shown in Table 2 [14]. The 4-RMS acceptance of HCEBIS is larger than that of the TEST EBIS by a factor of 2 due to mainly our estimated electron-beam radius being also larger by a comparable amount (see Eq. (4)). For the maximum geometrical acceptance, the difference of the acceptance is reduced because the electron-beam space-charge potential of the TEST EBIS is deeper than that of the HCEBIS. It is complementary to the smaller electron-beam radius.

Table 2: Acceptance Comparison

| | HCEBIS | TEST EBIS |
|--------------------------------------|-------------|-------------|
| Electron-beam radius | 0.796 mm | 0.55 mm |
| Electron-beam current | 4 A | 9 A |
| Ion injection potential | 12 keV | 22 keV |
| 4-RMS acceptance ($f_{overlap}=1$) | 167 mm·mrad | 81 mm·mrad |
| Maximum geometrical acceptance | 217 mm·mrad | 165 mm·mrad |

CHARGE BREEDER FOR HIGH INTENSITY BEAM

EBIT Operation for High-Intensity Ion Beams

To predict the capability of the HCEBIS, the production of high-intensity beams was tested and the electron-beam compensation ratio of the ReA EBIT was measured. When the BCB [4, 15] is operated in the pulsed mode for injection into the EBIT, the maximum beam rate capability is between 10^8 – 10^9 ejected ions per pulse. For the studies presented here, the BCB was operated in the continuous-injection mode to maximize the injected beam current. After optimization, a maximum Ne^{8+} beam rate after the Q/A separator of 1.748×10^{10} pps was obtained with a breeding time of 20 ms and a repetition rate of 33 Hz. The electron-beam current was set to 425 mA.

Figure 9 shows the optimized number of extracted Ne^{8+} ions as function of the number of ions ejected from the BCB. The number of extracted Ne^{8+} ions increases with the injected rate until it reaches a saturation limit. This could be explained by the electron-beam space-charge potential being largely neutralized and hence no longer efficiently confining and charge breeding injected ions.

Figure 10 shows a mass-over-charge (A/Q) scan performed during the tests. Ne^{8+} accounts for about 27 % of the total number of charge in the A/Q spectrum. Based on the achieved beam rate of 1.748×10^{10} pps in Fig. 9, the total charges of all extracted ion can be estimated as 1.569×10^{10} charges. With an electron-beam current of 425 mA, energy of 12 keV, and trap length of 0.635 m, the total charge ca-

capacity of the ReA EBIT is 2.587×10^{10} charges. If we assume a 10 % loss in beam transport, the compensation ratio is estimated as approximately 69 %. This value is comparable, but more than twice higher than the compensation ratio reported by the REXEBIS group as 30 % with injected $^{40}\text{Ar}^{+}$ beam [16]. With a current of 4 A, the charge capacity of the HCEBIS is higher than that of the ReA EBIT by factor of 10. Therefore, the HCEBIS is expected to be able to charge bred and produce intense beams exceeding 10^{11} pps.

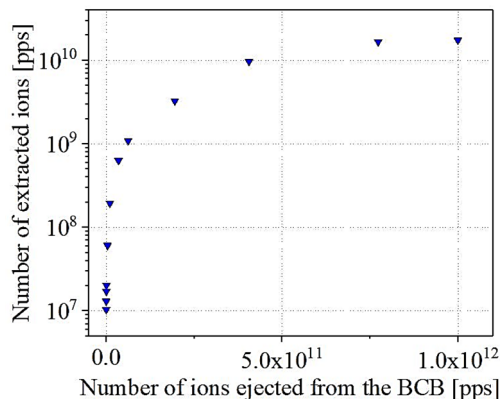


Figure 9: Ne^{8+} intensity after the Q/A separator.

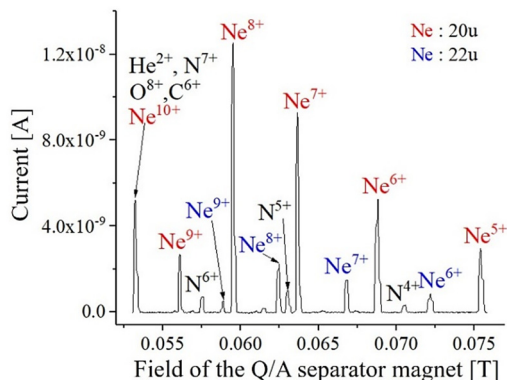


Figure 10: Mass-over-charge spectrum of highly charged ions resulting from external injection of.

CONCLUSION

A High-Current EBIS (HCEBIS) is being implemented for the ReA post-accelerator for charge breeding of intense beams. Over the last months, the cathode was tested in a test configuration up to 1.12 A. The beam acceptance and emittance were also simulated. To confirm the capability if the HCEBIS to handle high beam rates, the production of high-intensity beams of up to 10^{10} pps was studied with the ReA EBIT. Those studies confirm that the HCEBIS will be able to charge breed and produce intense beams exceeding 10^{11} pps. First transport if an electron-beam through its superconducting magnet and ion extraction is expected early next year.

ACKNOWLEDGEMENTS

This material is based on work supported by the National Science Foundation under Grant No. PHY-1565546.

REFERENCES

- [1] A. C. C. Villari, "Reacceleration of Rare Isotope Beams at Heavy-Ion Fragmentation Facilities," presented at EMIS-2018, Geneva, Switzerland, Sep. 2018.
- [2] J. Wei, "The Facility for Rare Isotope Beams," presented at APS April Meeting 2020, Washington D.C., MD, Apr. 2020.
- [3] H. Schatz *et al.*, "SEparator for CApture Reactions (SECAR) Pre-Conceptual Design Report," FRIB, East Lansing, USA, Rep. FRIB-M41600-RP-000055-R002, Oct. 2014.
- [4] A. Lapiere *et al.*, "First two operational years of the electron-beam ion trap charge breeder at the National Superconducting Cyclotron Laboratory," *Phys. Rev. Accel. Beams*, vol. 21, p. 053401, May 2018.
doi.org/10.1103/PhysRevAccelBeams.21.053401
- [5] E. N. Beebe *et al.*, "TEST EBIS Operation and Component Development for the RHIC EBIS," *Journal of Physics: Conference Series* 2, pp. 164–173, 2004.
doi:10.1088/1742-6596/2/1/020
- [6] A. Pikin, "EBIS for high intensity stable beams," *International Committee for Future Accelerators Beam Dynamics Newsletter*, no. 73, pp. 101-112, Apr. 2018.
- [7] Field Precision LLC, <http://www.fieldp.com>
- [8] F. Wenander *et al.*, "REXEBIS the Electron Beam Ion Source for the REX-ISOLDE Project Design and Simulation," CERN, Geneva, Switzerland, Rep. CERN-OPEN-2000-320, 1999.
- [9] G. Zachornack *et al.*, "Electron beam ion source," *Proceedings of the CAS-CERN Accelerator School*, CERN-2013-007, pp. 165-202, Senac, Slovakia, Dec. 2013.
doi:10.5170/CERN-2013-007
- [10] S. Schwarz *et al.*, "A high-current electron gun for the electron beam ion trap at the National Superconducting Cyclotron Laboratory," *Rev. Sci. Instrum.*, vol. 85, p. 02B705, 2014.
doi.org/10.1063/1.4827109
- [11] T. M. Baumann *et al.*, "Determination of the ReA Electron Beam Ion Trap electron beam radius and current density with an X-ray pinhole camera," *Rev. Sci. Instrum.*, vol. 85, p. 073302, 2014.
doi.org/10.1063/1.4885448
- [12] C. Dickerson *et al.*, "Simulation and design of an electron beam ion source charge breeder for the californium rare isotope breeder upgrade," *Phys. Rev. ST Accel. Beams*, vol. 16 p. 02420, 2013.
doi: 10.1103/PhysRevSTAB.16.024201
- [13] R. Baartman, "Emittance Convention," TRIUMF, Vancouver, Canada, Rep. TRI-BN-15-07, June 2015.
- [14] R. Kponou *et al.*, "Determining the acceptance of the Brookhaven EBIS test stand for primary ions by computer simulation," *Journal of physics: Conference Series* 2, pp. 165-172, 2014.
doi.org/10.1063/1.1148714
- [15] G. Bollen, "Beam Development," presented at SECAR Collaboration Meeting, MSU, East Lansing, MI, 2015.
- [16] J. Pitters *et al.*, "Summary of charge breeding investigations for a future 11C treatment facility," CERN, Geneva, Switzerland, Rep. CERN-ACC-NOTE-2018-0078, Nov. 2018.